JACS
JOURNAL OF THE AMERICAN CHEMICAL SOCIETY
Article
pubs.acs.org/JACS

Interfacial Effects on the Band Edges of Functionalized Si Surfaces in Liquid Water

Tuan Anh Pham,*[,†,‡] Donghwa Lee,[‡] Eric Schwegler,[‡] and Giulia Galli*[,§]

[†]Department of Chemistry, University of California, Davis, California 95616, United States
[‡]Lawrence Livermore National Laboratory, Livermore, California 94551, United States
[§]The Institute for Molecular Engineering, University of Chicago, Chicago, Illinois 60637, United States

Supporting Information

ABSTRACT: By combining *ab initio* molecular dynamics simulations and many-body perturbation theory calculations of electronic energy levels, we determined the band edge positions of functionalized Si(111) surfaces in the presence of liquid water, with respect to vacuum and to water redox potentials. We considered surface terminations commonly used for Si photoelectrodes in water splitting experiments. We found that, when exposed to water, the semiconductor band edges were shifted by approximately 0.5 eV in the case of hydrophobic surfaces, irrespective of the termination. The effect of the liquid on band edge positions of hydrophilic surfaces was much more significant and determined by a complex combination of structural and electronic effects. These include structural rearrangements of the semiconductor surfaces in the presence of water, changes in the orientation of interfacial water molecules with respect to the bulk liquid, and charge transfer at the interfaces, between the solid and the liquid. Our results showed that the use of many-body perturbation theory is key to obtain results in agreement with experiments; they also showed that the use of simple computational schemes that neglect the detailed microscopic structure of the solid−liquid interface may lead to substantial errors in predicting the alignment between the solid band edges and water redox potentials.

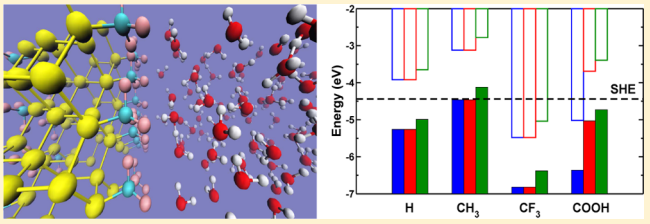

INTRODUCTION

The photocatalysis of water splitting is a promising way to capture and store solar energy and is an active research field.[1] In photoelectrochemical (PEC) cells, one harvests photons to create electron−hole pairs in semiconductor materials and uses these charge carriers in photoelectrochemical reactions to turn water into hydrogen and oxygen, which may then be used as chemical fuels.

The simplest way to build a PEC cell is to use a single semiconductor material with an appropriate band gap and band edge positions.[2] The optimal band gap of the solid should be larger than 1.9 eV (a value determined by the energy necessary to split water and inclusive of thermodynamic losses and overpotential) and smaller than 3.1 eV in order to fall within the visible range of the solar spectrum.[1,3] In addition, the semiconductor valence band maximum (VBM) and conduction band minimum (CBM) must straddle the water redox potentials to ensure the reactions are thermodynamically accessible upon photon absorption.

Alternatively, a potentially more efficient PEC design is based on two semiconductor−liquid junctions: an n-type semiconductor, for the photoanode where water oxidation occurs, and a p-type one, for the photocathode where water reduction takes place.[2,4] Each photoelectrode provides part of the water splitting potential, and thus semiconductors with smaller band gaps that absorb a larger fraction of the visible light can be utilized to improve the overall conversion efficiency of the device. For this design to work, the CBM of the photocathode must be higher than the water reduction potential H^+/H_2O, and the VBM of the photoanode, lower than the oxidation potential O_2/H_2O. Hence, irrespective of the scheme chosen to build a PEC cell, one of the critical factors to select candidate semiconductors for the electrodes is the alignment between their band edge positions and water redox potentials.

Accurate theoretical predictions of the alignment between photoeletrode band edges and water redox potentials require explicit calculations of the electronic properties of semiconductor−liquid interfaces. This is a challenging task, as it requires (i) realistic structural models of the interface and (ii) the calculation of electronic states of models composed of several hundreds of electrons using advanced electronic structure methods, such as density functional theory (DFT) with hybrid functionals[5] or many-body perturbation theory, e.g., within the GW approximation.[6] In particular, although hybrid functional[7,8] and GW calculations are now feasible for systems containing several hundreds of electrons,[9,10] they are rather demanding from a computational standpoint, especially for condensed systems, using periodic boundary conditions. Due to these difficulties, calculations of the alignment between photoelectrode band edges and water redox potentials usually involve several approximations, which are discussed below.

Received: August 4, 2014
Published: November 17, 2014

Most computational approaches used so far neglected the effects of the liquid on the semiconductor surface.[11−14] Band edge positions were simply computed in vacuum and aligned to the experimental values[15] of the water redox potentials. The neglect of solid−liquid interfaces allowed one to use supercells of moderate sizes, for which a high level of theory may be employed at a reasonable computational cost, e.g., the GW approximation to overcome DFT errors on band gaps and band edge positions. This computational procedure was adopted to investigate numerous candidate photoelectrode materials, including transition metal oxides (MnO, FeO, Fe_2O_3, NiO, Cu_2O)[11] and single layer transition metal dichalcogenides MX_2.[12,13]

An approach similar to that of refs 11−13 was recently employed to compute band edge positions of a set of 17 materials (both n-type and p-type) of interest for water splitting.[14] To address the effect of liquid water, the authors compared the band edges in vacuum with those measured electrochemically at the point of zero charge (PZC), and they suggested that the water−electrode interaction would simply amount to a band edge shift of approximately 0.5 eV, irrespective of the material.

Calculations that explicitly include a semiconductor−liquid interface have, to date, been rather sparse. Band edge positions of TiO_2 relative to the normal hydrogen electrode potential were computed in ref 16 using the solvation energy of the H^+ ion as reference. The electronic properties were obtained using DFT with a semilocal density functional, which yielded substantial errors on the band positions when compared to experimental values (errors of 0.4 and 1.6 eV for the CBM and VBM, respectively). Similar to ref 14, the authors showed that the interaction with water brings the TiO_2 band edge positions closer to the vacuum level, but with a significantly larger shift (∼2.0 eV).

Explicit calculations for semiconductor−liquid interfaces were also reported in ref 17 for six photocatalyst materials (TiO_2, WO_3, CdS, ZnSe, GaAs, and GaP). The authors aligned the band edges of these systems with the lowest unoccupied molecular orbital (LUMO) of the H_3O^+ ion, present in a sample of liquid water put in contact with the semiconductor; they used DFT with semilocal functionals and assumed that cancellation of errors would occur between the values obtained for the band positions and the LUMO of the hydronium ion. Computational procedures to generate interfacial models were not discussed in ref 17. As pointed out in the Results and Discussion section, the surface structure may significantly affect the semiconductor band edge positions and their alignment with the water redox potentials.

In this paper, we present first-principles calculations of the absolute band edge positions of functionalized Si(111) surfaces in contact with liquid water and predictions of their alignment with water redox potentials. At variance with most approaches presented so far in the literature, we explicitly took into account the interaction of liquid water and the semiconductor surfaces by generating realistic interfacial models with *ab initio* molecular dynamics (MD); in addition we computed the electronic states using many-body perturbation theory, within the GW approximation. We considered the hydrogen terminated Si(111) surface, for which many measurements are available for comparison,[18,19] and several additional terminations used experimentally to functionalize p-type Si photoelectrodes for water splitting. In particular we investigated CH_3-, CF_3-, and COOH-terminated Si(111) surfaces, as chemically stable Si−C bonds were shown to passivate Si surfaces both electrically and chemically, while allowing for secondary functionalization of the electrodes.[20−23] Thus, in our work we considered both hydrophobic (H-, CH_3-, CF_3-terminated) and hydrophilic (COOH-terminated) substrates.

In agreement with ref 24, our calculations showed that surface termination strongly influenced the electronic structure of the solid; i.e., the band edge positions of the Si(111) surface may vary as much as 1.5 eV as a function of termination. Hence a favorable alignment of semiconductor band edges and water redox potential for water splitting applications may be achieved by engineering the surface termination of the semiconductor.

Most importantly, our simulations revealed the effect of interfacial water molecules on the electronic states of the semiconductor surfaces. For the three hydrophobic substrates, we found that the presence of the liquid amounts to similar shifts of the semiconductor band edges obtained in vacuum, on the order of 0.5 eV; these results indicate that in materials screening studies of hydrophobic substrates, if an accuracy less than 0.5 eV is acceptable, no explicit inclusion of water is necessary. In contrast, we observed a dramatic effect of water on the band edges of the hydrophilic COOH-terminated Si(111) surface, with the band edge shift on the order of 1.5 eV. We found the shift was determined by several factors including the structural rearrangements of the semiconductor surface, the orientation of interfacial water molecules, and the charge transfer between the liquid and the solid occurring at the interface. Our results showed that the use of simple computational schemes neglecting the complex solid−liquid interaction may lead to substantial errors in predicting photoelectrode band edges in the case of hydrophilic substrates. This includes not only the specific case of functionalized photocathodes studied here in detail but also all oxide and nitride materials used as photoanodes.

The rest of the paper is organized as follows. In section 2 we outline our computational strategy, in particular our approach to evaluate the absolute band edge positions of a semiconductor in liquid water. In section 3 we present results for Si(111)−water interfaces, and we discuss the effect of water on the solid band edges, as well as comparisons with experimental results when available. Our conclusions and outlook are presented in section 4.

METHODS

We developed a computational strategy to determine the band edges of a semiconductor in the presence of liquid water, with respect to vacuum and to the standard hydrogen electrode (SHE), which consisted of the following steps: (i) we generated realistic models of the solid−liquid interfaces by *ab initio* MD simulations; (ii) we computed the band offsets at the solid−liquid interfaces with many-body corrections obtained within the G_0W_0 approximation based on DFT eigenvalues and orbitals;[25] and (iii) finally, knowing the absolute positions of the water band edges, as determined at the same level of theory in our recent study,[26] we obtained the absolute position of the semiconductor band edges with respect to vacuum and to the SHE, inclusive of the complex effects induced by liquid water on the solid surface. To the best of our knowledge this computational procedure, which is general and applicable to any nonmetallic surface in contact with water, has not been reported before in the literature. Additional details of our computational strategy are given in the Supporting Information.

We chose to carry out calculations of the electronic states using many-body perturbation theory within the G_0W_0 approximation for several reasons: (i) previous work[26,27] showed that the band gaps and band edge positions of liquid water and bulk Si computed with the

dx.doi.org/10.1021/ja5079865 | J. Am. Chem. Soc. 2014, 136, 17071−17077

G_0W_0 approximation were in good agreement with experimental results; (ii) calculations with hybrid functionals, although computationally less demanding, yield results for electronic levels that depend on the mixing parameter chosen for the Hartree−Fock exchange;[28] such parameters are system dependent, and there is no known functional yielding accurate results for interfaces composed of materials with dielectric properties as different as those of water ($\epsilon_0 \approx 1.78$[26]) and Si ($\epsilon_0 \approx 11.7$[27]); and (iii) despite recent progress in wave function methods for periodic systems,[29] these are not yet applicable to the size of systems and type of problems tackled in this work.

Our G_0W_0 calculations were made possible by a newly developed algorithm[9,10] that is applicable to systems with hundreds of electrons. At variance with all conventional G_0W_0 approaches used in the literature of the past several decades, such an algorithm does not require the explicit evaluation of virtual electronic states. In addition, the accuracy of the results is controlled by a single parameter, i.e., the number of basis functions included in the spectral decomposition of the static dielectric matrix. Additional details of our G_0W_0 calculations are given in the Supporting Information.

The Si−water interfacial models considered in this work consisted of 108 water molecules and a six-layer slab of 72 Si atoms representing the Si(111) surface at the theoretical lattice constant of a = 5.48 Å. We considered full adsorbate coverage for all surfaces; experimentally, the maximum coverage obtained for the COOH-terminated Si(111) substrate is ∼0.5,[30] with the rest of the surface Si atoms terminated by H atoms; hence our results are representative of a model hydrophilic surface.

Car−Parrinello MD simulations,[31] where all water molecules and atoms of the semiconductor surfaces were allowed to readjust, were carried out with the Quantum-ESPRESSO code[32] using DFT with the Perdew−Burke−Ernzerhof (PBE) approximation for the exchange-correlation functional.[33] We used an effective electronic mass of μ = 340 au, which was shown to yield the same results obtained with Born−Oppenheimer MD simulations of liquid water, in which the electronic ground state wave functions were optimized at each ionic step.[34,35] We employed ultrasoft pseudopotentials, with electronic wave functions and charge densities expanded in a plane-wave basis set truncated at a cutoff energy of 25 and 180 Ry, respectively. Our simulations were carried out at a constant temperature (NVT conditions) of T = 375 K for ∼30 ps for each interface. An elevated simulation temperature was used to recover the experimental structure and diffusion coefficients of liquid water at T = 300 K, as the neglect of quantum zero-point motion effects of light nuclei and the use of the PBE approximation are known to yield an overstructured liquid in *ab initio* simulations of water.[34,35] Further information on the structural and dynamical properties of water molecules at the interfaces considered in this work can be found in ref 36.

RESULTS AND DISCUSSION

Band Edges of Si Surfaces in Vacuum and Water. Figure 1 shows the VBM (filled rectangles) and CBM (empty rectangles) positions of different functionalized Si(111) surfaces, computed at the G_0W_0 level of theory, following the procedure described in the previous section. We present results obtained for the surfaces in vacuum (blue) and in the presence of liquid water (green). In addition we show the energy levels (red) computed in the absence of the liquid, but for surface geometries determined in the presence of water.

We first compared the band edges obtained for the surfaces in vacuum (blue) to the ionization potential (IP) measured in photoemission experiments in the absence of water. Experimental results were available for the H− and CH_3−Si(111) surfaces, and we obtained IP values of 4.76 and 3.96 eV with DFT and the PBE functional, which severely underestimated the experimental data of 5.29 and 4.76 eV,[20,24] respectively. The use of G_0W_0 many-body corrections significantly improved the agreement with measurements, yielding 5.26 and 4.46 eV, respectively. For details see Table S1 and Figure S4 in the Supporting Information.

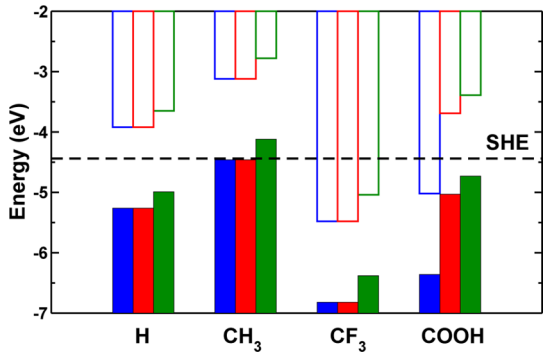

Figure 1. Valence band maxima (filled rectangles) and conduction band minima (empty rectangles) of the Si(111) surface functionalized with various groups indicated on the x-axis, as computed with the G_0W_0 approximation. We considered three cases: silicon−vacuum interfaces, with surface geometries optimized without water (blue rectangles); silicon−vacuum interfaces, with surface geometries extracted from MD trajectories performed in the presence of water (red rectangles); silicon−water interfaces, with results obtained by averaging values computed for several snapshots extracted from *ab initio* MD trajectories (green rectangles). The dashed line shows the experimental value of the standard hydrogen potential (SHE).

We then compared band edges of the H−Si(111) surface in liquid water (green) to electrochemical experiments at the PZC. We obtained CBM and VBM positions of 3.65 and 4.99 eV below the vacuum level with the G_0W_0 approximation, in satisfactory agreement with experimental results of 3.98 and 5.1 eV, respectively[18] (for details see Table S2 and Figure S4 in the Supporting Information); these findings indicate that many-body perturbation theory yields quantitative agreement with measurements not only for surfaces in vacuum but also for complex interfaces, such as those with liquid water. Note (Figure S4) the qualitative difference between some of the DFT and G_0W_0 results: for example, in the absence of water, the valence band of the CH_3−Si(111) surface is above the SHE within DFT but below the value of the SHE when computed with G_0W_0. In the presence of water, the valence band of the COOH−Si(111) surface is above the SHE within DFT but below the SHE within G_0W_0.

As expected, we found that the absolute band edge positions of Si(111) surfaces in water strongly depend on the termination. In particular, the CBM of the H- and CH_3-terminated Si(111) surfaces are higher than the SHE, while that of the CF_3-terminated Si(111) surface is lower. Our calculations predicted that the hydrophilic COOH-terminated surface exhibits a slight shift (∼0.25 eV) of the band edges compared to those of the H-terminated one, and its CBM is higher than the SHE.

Alignment with the water redox potentials requires additional knowledge of the PZC, as water redox potentials at room temperature vary as a function of the pH, following the Nernst equation:[37]

$$E_{red}^{pH} = E_{red}^{pH=0} - 0.059 \times pH \quad (1)$$

where E_{red}^{pH} is the redox potential measured on the SHE scale. However, qualitative conclusions may be drawn. The CBM of the H−Si(111) surface is higher than the water reduction potential at the PZC (∼2.2),[18] and thus it is suitable for

dx.doi.org/10.1021/ja5079865 | J. Am. Chem. Soc. 2014, 136, 17071−17077

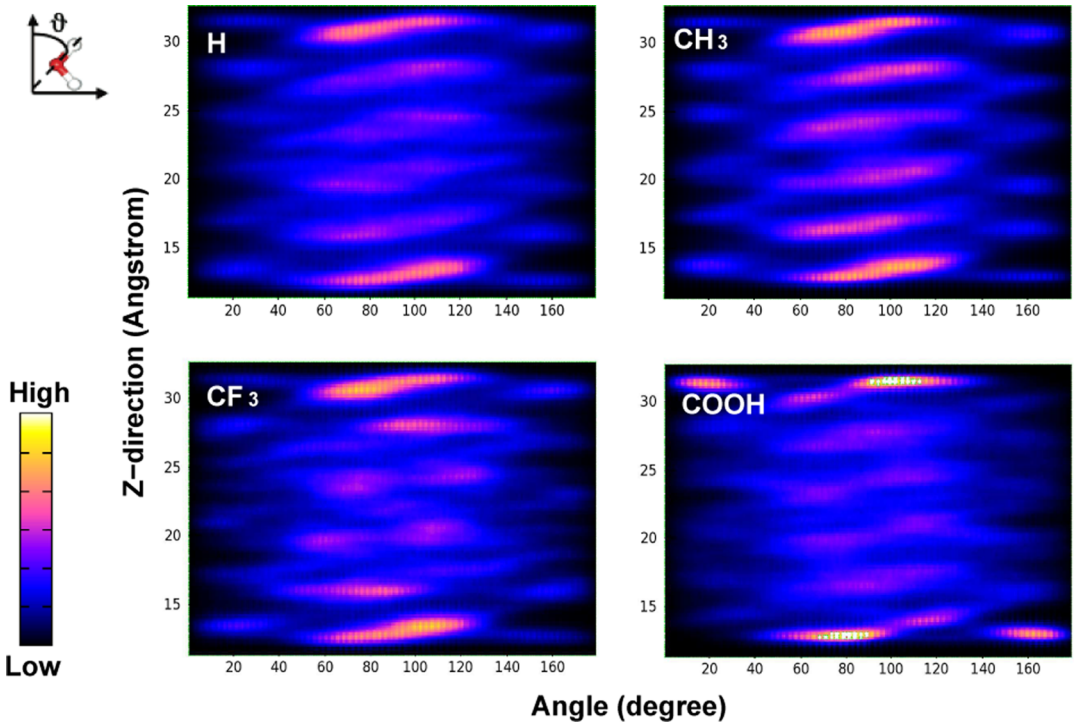

Figure 2. Probability of finding given OH bond vector orientations as a function of the distance from the outermost surface Si atoms, computed for H-, CH_3-, CF_3-, and COOH-terminated Si(111) surfaces.

hydrogen evolution. The same conclusion holds for the CH_3- and COOH-terminated surfaces, as their CBM positions are higher than the water reduction potential at any pH value in the range of 0−14. The CF_3-terminated surface is instead not suitable for the hydrogen evolution reaction, as its CBM position is always lower than the water reduction potential. However, this surface could be suitable for the oxygen evolution reaction, as its VBM position is lower than the water oxidation potential at any pH value.

Finally we note that our results indicate the hydrophobic H−Si(111) and hydrophilic COOH−Si(111) surfaces yield similar band edge positions. However, this similarity does not at all imply that the effect of water on the atomistic and electronic structure of the two surfaces is similar. In fact both water reorientation and charge transfer are profoundly different in the two cases, but eventually they lead to similar band edge positions for the reasons that we discuss below.

Impact of Interfacial Effects. We found that the presence of liquid water alters the solid band edges computed in vacuum in several important ways: (i) water may modify the solid surface structure and hence the effective surface dipole; and (ii) interfacial water molecules may form an additional dipole layer, counteracting or enhancing the solid surface dipole. We emphasize that the understanding of both effects was possible, as our computational strategy fully included interfacial effects. In particular, the comparison between blue and red rectangles in Figure 1 highlights the effect of the structural modifications caused by the presence of the liquid on the electronic states of the surface in vacuum. The difference between red and green rectangles reveals instead the effect of the interfacial dipole arising from the solid−liquid interaction on the calculated band edges.

For the three hydrophobic surfaces, we found negligible differences between results obtained for geometries optimized in the absence of liquid water (blue rectangles) and those computed for configurations extracted from MD simulations (red rectangles). This result indicates that hydrophobic Si(111) surface structures are weakly affected by the presence of water. The inclusion of the interfacial dipole shifts the band edge positions closer to the vacuum level by ∼0.3−0.5 eV (see blue and green rectangles), and such a small difference is consistent with the rather weak surface water interaction. Overall, our analysis showed that if the accuracy required in screening surfaces or optimal photoelectrodes is within 0.5 eV, the effect of the solution may be neglected in the case of hydrophobic surfaces.

In contrast, we found that both surface structure modification and solid−liquid interaction play key roles in the case of the hydrophilic COOH−Si(111) surface. In particular, band edges computed with the surface geometry extracted from MD trajectories are shifted significantly closer to vacuum (∼1.3 eV), when compared to those determined without liquid water. This analysis clearly indicates that the electronic structure of hydrophilic surfaces may be strongly modified in the presence of the liquid. In addition to surface modification, our calculations showed that the interfacial dipole arising from the solid−liquid interaction further shifts the band edge of the COOH-terminated Si(111) surface closer to vacuum by ∼0.3 eV, i.e., an amount similar to that found for hydrophobic surfaces. Hence the magnitude and direction of the COOH−Si(111) band edge shift could be interpreted as a signature of interfacial water molecules with similar molecular dipole moments and orientations for both hydrophobic and hydrophilic surfaces. As shown below, this interpretation is incorrect and the understanding of our results requires a more complex analysis.

In order to investigate the molecular dipole moment of interfacial water molecules, we computed the OH bond tilt angle (θ), defined as the angle that a vector along an OH bond forms with the direction perpendicular to the surface (see

dx.doi.org/10.1021/ja5079865 | J. Am. Chem. Soc. 2014, 136, 17071−17077

Figure 2). The probability distribution of θ as a function of the angle and the distance from the outermost surface Si atom is shown in Figure 2.

We found that the three hydrophobic surfaces exhibit similar angular probability distributions which are consistent with that computed for water in hydrophobic confinement.[38] In particular, at about ~2.1 Å from the surfaces, the angular probability distribution shows a strong peak at 60° and a weak one at 160°: these orientations correspond to OH bonds pointing slightly outward from and toward the surface, respectively. This indicates that the dipoles of interfacial water molecules tend to point away from the hydrophobic surfaces. Our results were further validated by examining the probability of specific molecular orientations at the interface (see Figure 3). The formation of an interfacial water layer with

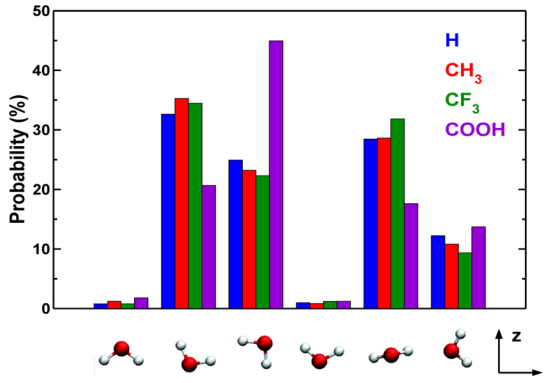

Figure 3. Probability of finding specific orientations of water molecules in the interfacial region between water and the Si (111) surfaces with termination indicated in the inset. The orientations were classified in six different categories, depending on the molecular dipole orientation with respect to the z-direction perpendicular to the surfaces. Note similar qualitative features for the three nonpolar surfaces.

a positive dipole thus accounts for the shift toward the vacuum level of the band edges of hydrophobic surfaces in the presence of water.

The orientation of water molecules at the interface with the hydrophilic COOH−Si(111) surface exhibits a noticeably different character. Figure 2 indicates that, in addition to a peak around 70°, the OH bond distribution shows a strong peak at 160°. Furthermore, the dipole moments of interfacial water molecules are preferably oriented toward the surface (maroon rectangles in Figure 3); i.e., the orientation of the dipole moments is opposite to that found in the case of hydrophobic surfaces.

Such differences in dipole orientation would appear to be at odds with the similar shifts of band edges toward the vacuum level, when taking into account the interfacial dipole, reported in Figure 1 for, e.g., H− and COOH−Si(111). We then further examined the electronic density at the interface; in particular, we computed:

$$\Delta\rho_e = \rho_e(\text{solid/liquid}) - \rho_e(\text{solid}) - \rho_e(\text{liquid}) \qquad (2)$$

The quantity $\Delta\rho_e$ is positive when there is an addition of charge to the system with respect to the isolated fragments and negative in the opposite case.

In Figure 4, we plot the planar average electronic density difference $\Delta\rho_e$ for a particular snapshot of the COOH−Si(111)/water interface. The main changes in the charge

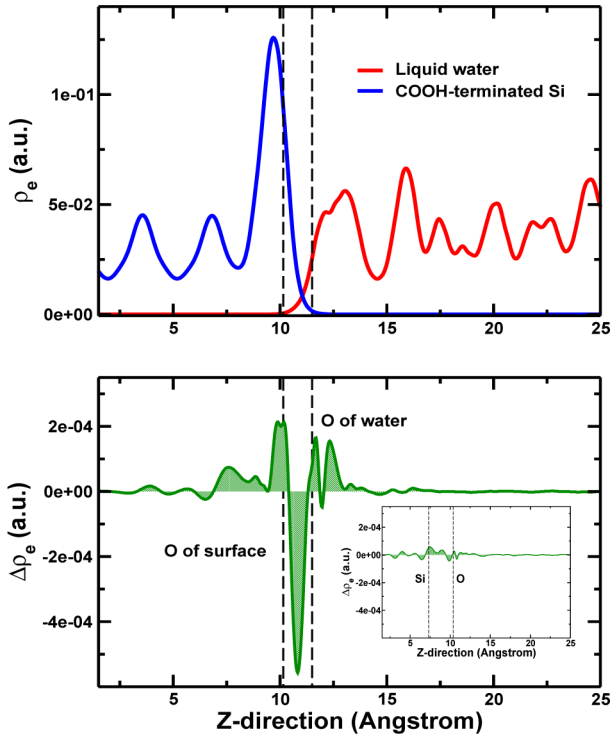

Figure 4. Charge transfer (see eq 2) at the COOH-terminated Si(111)−water interface as a function of the distance from the interface (z) in the direction perpendicular to the interface. The inset shows the same quantity computed for the H-terminated Si(111)−water interface.

density are localized directly at the interface, and there is a charge transfer from liquid water toward the semiconductor. This charge transfer leads to the creation of an additional dipole layer with a positive dipole moment that shifts the solid band edges closer to vacuum. In the case of the COOH-terminated surface, the charge transfer is clearly more significant than that for the H-terminated one (inset of Figure 4) and over-compensates the effect of the intrinsic dipole moment of the water layer, leading to a net shift closer to vacuum. A similar behavior was observed for the work function of metals, e.g., Pt and Ru, interfaced with water.[39] Thus, the effect of the liquid on the band edges of the hydrophilic COOH− surface arises from the complex and subtle combination of the structural rearrangement of the semiconductor surface, the molecular dipole of interfacial water molecules, and charge transfer at the interface.

CONCLUSIONS

We devised a computational strategy to compute, from first-principles, band edge positions of semiconductors and insulators interfaced with liquid water, with respect to vacuum and to water redox potentials. In particular, we combined *ab initio* molecular dynamics simulations of structural properties with many-body perturbation theory calculations of electronic energy levels. The computational approach employed in this work explicitly takes into account the effect of the solid−liquid interaction, including structural rearrangements occurring at the interface and finite temperature effects. The method presented here has general applicability, and it may be adopted in any problem where a determination of electronic states at the interface between a liquid and a nonmetallic surface is required,

dx.doi.org/10.1021/ja5079865 | J. Am. Chem. Soc. 2014, 136, 17071−17077

e.g., in batteries or in nanocomposites in solution, for solar cells.

Our results showed that the use of GW calculations enables one to obtain band edge positions that are in good agreement with experiments for both Si(111) surfaces in vacuum and in the presence of liquid water. Similar to experiments and previous studies,[24] we found that band edge positions of Si and their alignment with water redox potentials are strongly dependent on the surface functionalization.

Most importantly, we showed that, in the presence of water, band edges of hydrophobic Si surfaces were shifted by approximately 0.5 eV, with respect to their respective values in vacuum and that these shifts were similar in sign and magnitude for all the surfaces, irrespective of functionalization. In contrast, in the case of hydrophilic substrates, the effect of water on the band edges of the semiconductor was much more substantial and determined by a combination of complex structural and electronic effects. We found that band edge shifts were determined by several factors, including the structural rearrangement of the solid surface, the molecular dipole moment of interfacial water molecules, and the charge transfer at the solid−liquid interfaces. Hence our results allowed us to establish clear connections between structural and electronic properties of the surfaces and their band alignment with vacuum and water redox potentials. Our findings also indicated that computational schemes neglecting the atomistic and electronic structure of aqueous interfaces may lead to substantial errors in the prediction of promising materials to be used as photoelectrodes for water splitting.

Finally we note that all results presented here correspond to electrochemical measurements at the PZC; work is in progress to compute band edge alignments of photoelectrodes in contact with water under different pH conditions, and with water with dissolved ions.[7,40]

■ ASSOCIATED CONTENT

Supporting Information

Methods to compute semiconductor band edges; details of GW and band edge calculations; geometical coordinates; additional tables and figures; structures. This material is available free of charge via the Internet at http://pubs.acs.org.

■ AUTHOR INFORMATION

Corresponding Authors

pham16@llnl.gov
gagalli@uchicago.edu

Notes

The authors declare no competing financial interest.

■ ACKNOWLEDGMENTS

We thank Prof. N. S. Lewis, Dr. T. Ogitsu, and Dr. B. Wood for useful discussions. Part of this work was performed under the auspices of the U.S. Department of Energy by Lawrence Livermore National Laboratory under Contract DE-AC52-07NA27344; part of this work was supported by DOE/BES (Grant No. DE-SC0008938) and NSF-CHE-0802907. T.A.P. acknowledges support from the Lawrence Scholar program.

■ REFERENCES

(1) McKone, J. R.; Lewis, N. S.; Gray, H. B. *Chem. Mater.* **2013**, *26*, 407−414.
(2) Walter, M. G.; Warren, E. L.; McKone, J. R.; Boettcher, S. W.; Mi, Q.; Santori, E. A.; Lewis, N. S. *Chem. Rev.* **2010**, *110*, 6446−6473.
(3) Ping, Y.; Rocca, D.; Galli, G. *Chem. Soc. Rev.* **2013**, *42*, 2437−2469.
(4) Grätzel, M. *Nature* **2001**, *414*, 338−344.
(5) Marsman, M.; Paier, J.; Stroppa, A.; Kresse, G. *J. Phys.: Condens. Matt.* **2008**, *20*, 064201.
(6) Onida, G.; Reining, L.; Rubio, A. *Rev. Mod. Phys.* **2002**, *74*, 601.
(7) Zhang, C.; Pham, T. A.; Gygi, F.; Galli, G. *J. Chem. Phys.* **2013**, *138*, 181102.
(8) Wan, Q.; Spanu, L.; Gygi, F.; Galli, G. *J. Phys. Chem. Lett.* **2014**, *5*, 2562−2567.
(9) Nguyen, H.-V.; Pham, T. A.; Rocca, D.; Galli, G. *Phys. Rev. B* **2012**, *85*, 081101.
(10) Pham, T. A.; Nguyen, H.-V.; Rocca, D.; Galli, G. *Phys. Rev. B* **2013**, *87*, 155148.
(11) Toroker, M. C.; Kanan, D. K.; Alidoust, N.; Isseroff, L. Y.; Liao, P.; Carter, E. A. *Phys. Chem. Chem. Phys.* **2011**, *13*, 16644−16654.
(12) Jiang, H. *J. Phys. Chem. C* **2012**, *116*, 7664−7671.
(13) Zhuang, H. L.; Hennig, R. G. *J. Phys. Chem. C* **2013**, *117*, 20440−20445.
(14) Stevanović, V.; Lany, S.; Ginley, D. S.; Tumas, W.; Zunger, A. *Phys. Chem. Chem. Phys.* **2014**, *16*, 3706−3714.
(15) Trasatti, S. *Pure Appl. Chem.* **1986**, *58*, 955.
(16) Cheng, J.; Sprik, M. *Phys. Rev. B* **2010**, *82*, 081406.
(17) Wu, Y.; Chan, M. K. Y.; Ceder, G. *Phys. Rev. B* **2011**, *83*, 235301.
(18) Madou, M.; Loo, B.; Frese, K.; Morrison, S. R. *Surf. Sci.* **1981**, *108*, 135−152.
(19) Higashi, G.; Chabal, Y.; Trucks, G.; Raghavachari, K. *Appl. Phys. Lett.* **1990**, *56*, 656−658.
(20) Hunger, R.; Fritsche, R.; Jaeckel, B.; Jaegermann, W.; Webb, L. J.; Lewis, N. S. *Phys. Rev. B* **2005**, *72*, 045317.
(21) Royea, W. J.; Juang, A.; Lewis, N. S. *Appl. Phys. Lett.* **2000**, *77*, 1988−1990.
(22) Plass, K. E.; Liu, X.; Brunschwig, B. S.; Lewis, N. S. *Chem. Mater.* **2008**, *20*, 2228−2233.
(23) OLeary, L. E.; Johansson, E.; Brunschwig, B. S.; Lewis, N. S. *J. Phys. Chem. B* **2010**, *114*, 14298−14302.
(24) Li, Y.; O Leary, L. E.; Lewis, N. S.; Galli, G. *J. Phys. Chem. C* **2013**, *117*, 5188−5194.
(25) Hybertsen, M. S.; Louie, S. G. *Phys. Rev. Lett.* **1985**, *55*, 1418.
(26) Pham, T. A.; Zhang, C.; Schwegler, E.; Galli, G. *Phys. Rev. B* **2014**, *89*, 060202.
(27) Pham, T. A.; Li, T.; Nguyen, H.-V.; Shankar, S.; Gygi, F.; Galli, G. *Appl. Phys. Lett.* **2013**, *102*, 241603.
(28) Skone, J. H.; Govoni, M.; Galli, G. *Phys. Rev. B* **2014**, *89*, 195112.
(29) Booth, G. H.; Grüneis, A.; Kresse, G.; Alavi, A. *Nature* **2013**, *493*, 365−370.
(30) Faucheux, A.; Gouget-Laemmel, A. C.; Henry de Villeneuve, C.; Boukherroub, R.; Ozanam, F.; Allongue, P.; Chazalviel, J.-N. *Langmuir* **2006**, *22*, 153−162.
(31) Car, R.; Parrinello, M. *Phys. Rev. Lett.* **1985**, *55*, 2471.
(32) Giannozzi, P.; Baroni, S.; Bonini, N.; Calandra, M.; Car, R.; Cavazzoni, C.; Ceresoli, D.; Chiarotti, G.; Cococcioni, M.; Dabo, I. M.; Dal Corso, A.; de Gironcoli, S.; Fabris, S.; Fratesi, G.; Gebauer, R.; Gerstmann, U.; Gougoussis, C.; Kokalj, A.; Lazzeri, M.; Martin-Samos, L.; Marzari, N.; Mauri, F.; Mazzarello, R.; Paolini, S.; Pasquarello, A.; Paulatto, L.; Sbraccia, C.; Scandolo, S.; Sclauzero, G.; Seitsonen, A. P.; Smogunov, A.; Umari, P.; Wentzcovitch, R. M. *J. Phys.: Condens. Matt.* **2009**, *39*, 395502.
(33) Perdew, J. P.; Burke, K.; Ernzerhof, M. *Phys. Rev. Lett.* **1996**, *77*, 3865.
(34) Grossman, J. C.; Schwegler, E.; Draeger, E. W.; Gygi, F.; Galli, G. *J. Chem. Phys.* **2004**, *120*, 300−311.
(35) Schwegler, E.; Grossman, J. C.; Gygi, F.; Galli, G. *J. Chem. Phys.* **2004**, *121*, 5400−5409.
(36) Lee, D.; Schwegler, E.; Kanai, Y. *J. Phys. Chem. C* **2014**, *118*, 8508−8513.

(37) Bolts, J. M.; Wrighton, M. S. *J. Phys. Chem.* **1976**, *80*, 2641−2645.
(38) Cicero, G.; Grossman, J. C.; Schwegler, E.; Gygi, F.; Galli, G. *J. Am. Chem. Soc.* **2008**, *130*, 1871−1878.
(39) Schnur, S.; Groß, A. *New J. Phys.* **2009**, *11*, 125003.
(40) Opalka, D.; Pham, T. A.; Sprik, M.; Galli, G. *J. Chem. Phys.* **2014**, *141*, 034501.